Caffeine removal from synthetic wastewater using magnetic fruit peel composites: Material characterization, isotherm and kinetic studies

Article · October 2021

DOI: 10.1016/j.envc.2021.100343

CITATIONS
0

READS
35

4 authors, including:

Cristina Almeida
Escuela Politécnica Nacional
20 PUBLICATIONS **37** CITATIONS
SEE PROFILE

María Belén
Escuela Politécnica Nacional
14 PUBLICATIONS **22** CITATIONS
SEE PROFILE

Victor Hugo Guerrero
Escuela Politécnica Nacional
71 PUBLICATIONS **341** CITATIONS
SEE PROFILE

Environmental Challenges 5 (2021) 100343

Contents lists available at ScienceDirect

Environmental Challenges

journal homepage: www.elsevier.com/locate/envc

Caffeine removal from synthetic wastewater using magnetic fruit peel composites: Material characterization, isotherm and kinetic studies

Cristina E. Almeida-Naranjo[a,*], María Belén Aldás[b], Génesis Cabrera[b], Victor H. Guerrero[c,*]

[a] Department of Mechanical Engineering, Escuela Politécnica Nacional, Ladrón de Guevara E11-253, Quito 170525, Ecuador
[b] Department of Civil and Environmental Engineering, Escuela Politécnica Nacional, Ladrón de Guevara E11-253, Quito 170525, Ecuador
[c] Department of Materials, Escuela Politécnica Nacional, Ladrón de Guevara E11-253, Quito 170525, Ecuador

ARTICLE INFO

Keywords:
Banana peel
Orange peel
Magnetite
Adsorption
Emerging contaminant

ABSTRACT

This work investigated the adsorption capacity of banana and orange peels, magnetite and their corresponding magnetic composites in the removal of caffeine from synthetic wastewater. The characteristics of the adsorbents were studied using proximal analysis, Fourier transform infrared spectroscopy (FT-IR), Raman spectroscopy, scanning electron microscopy (SEM), energy dispersive spectroscopy (EDS), Brunauer, Emmett and Teller (BET) analysis and X-ray diffraction. Batch adsorption tests were conducted to determine the influence of the adsorbent dose (0.5 and 10.0 g/L), contact time (5 – 180 min) and initial caffeine concentration (10 – 50 mg/L) in the caffeine removal. The fittings of the experimental data to the pseudo first order, pseudo second order, Elovich, and diffusion kinetic models, as well as to the Langmuir, Freundlich and Sips isotherm models were also studied. The use of magnetic peels improved around 1.7 times the adsorption capacity of peels. The effective doses were 3.5 g/L of orange peel, 9.5 g/L of banana peel, 2.5 g/L of orange peel composite, 5.5 g/L of banana peel composite, and 5 g/L of magnetite, achieving caffeine removal efficiencies of 95.5 ± 0.3%, 90.5 ± 0.5%, 93.6 ± 0.2%, 89.2 ± 0.01% and 54.8 ± 0.8%, respectively. The adsorption using the peels, magnetite, and their magnetic composites better fitted the pseudo first order kinetic model and the Langmuir and Sips isotherm models.

1. Introduction

The availability of clean water is not only essential for life, but it is also of crucial importance for social and economic development. Paradoxically, this same development and the growth of the population demand the consumption of larger amounts of water (4600 km^3/year) and are related to its contamination and subsequent impacts (Boretti and Rosa, 2019). During the last few decades, the potential environmental impacts of a series of new anthropogenic contaminants has attracted the attention of the scientific community and public in general. These so-called “emerging contaminants” (ECs) include pharmaceuticals, personal care products, endocrine disrupting compounds, illegal drugs, among others. These substances have been found in water bodies and wastewater in concentrations between ng/L and μg/L (e.g. pharmaceuticals between 0.02 ng/L to 50.00 μg/L). Several studies determine that ECs are both potentially toxic and very persistent, and they can directly or indirectly affect several organisms due to bioaccumulation and biomagnification (Quesada et al., 2019). Besides this, their removal is not effectively performed in conventional wastewater treatment plants (WWTPs). Conventional mechanical – biological WWTPs were used achieving an efficiency around 60% (Kot-Wasik et al., 2016). Therefore, it is desirable and necessary to improve the traditionally used treatment technologies and to develop non-conventional technologies. The efforts in this sense must consider not only the performance that needs to be achieved but also the capital and technology requirements (Shah et al., 2020).

Caffeine is a stimulant of the central nervous system, present in drinks such as coffee, tea, soft drinks, and energy drinks; becoming one of the most widely consumed pharmaceuticals (177.7 mg/person/day) (Korekar et al., 2019). Caffeine has been found in the WWTP influents and effluents (0.1 to 20 μg/L), in groundwater (10 to 80 ng/L), and in rivers, lakes and sea water (3 to 1500 ng/L) (Álvarez-Torrellas et al., 2016). The presence of caffeine in aquatic ecosystems represents a risk for biota (e.g. zebra fish, *Mytilus californianus, Ruditapes philippinarum, Carcinusmaenas,* etc.) due to its physicochemical properties and its chronic toxicity (Korekar et al., 2019). Therefore, the search for alternatives to remove caffeine from wastewater is important. Treatments such as biochemical degradation, photolysis, reverse osmosis, ozonation, advanced oxidation and adsorption process are used in the caffeine removal (Sotelo et al., 2014).

* Corresponding author.
E-mail addresses: cristina.almeidan@epn.edu.ec (C.E. Almeida-Naranjo), victor.guerrero@epn.edu.ec (V.H. Guerrero).

https://doi.org/10.1016/j.envc.2021.100343
Received 30 August 2021; Received in revised form 17 October 2021; Accepted 19 October 2021

Adsorption is an economical, easy-to-implement, highly efficient and environmentally friendly process to remove various types of contaminants. One of the most widely used and marketed adsorbent materials is activated carbon; but its cost (20 – 22 USD/kg) could limit its use at large scale (Sotelo et al., 2014; Portinho et al., 2017). Several non-conventional adsorbents have been used in the removal of emerging contaminants, including heavy metals, from aqueous environments (Zamora-Ledezma et al., May 2021). For instance, fungal strains biomass for Pb(II) ion removal and inactive bacterial strains biomass for Cd(II) ion removal were used, achieving high efficiencies (Zamora-Ledezma et al., May 2021; Long et al., 2019). Other adsorbent materials used for the caffeine removal from solutions and real wastewater were polymeric resins, nanomaterials, carbon nanotubes, biochar, modified graphite sheets, zeolites, aluminosilicates, among others. Furthermore, organic, lignocellulosic or agro-industrial residues (husk, shells, peels, leaves or fruit seeds, stalks) and new generation adsorbents (nanoparticles and composites) are also presented as an alternative (Bachmann et al., 2021). In any case, the adsorbent material used should exhibit desirable characteristics such as selectivity, high surface area, high adsorption capacity, low cost, long service life, and recyclability (Rigueto et al., 2020). Agro-industrial residues are available at low or no cost, and have a porous surface with the presence of functional groups that improves the adsorption process (Portinho et al., 2017). In particular, around 12.0 to 20.8 tons of orange peels and 35.4 to 47.2 million tons of banana peels are produced annually worldwide, and do not have a defined use (Portinho et al., 2017; Martínez-Ruano et al., 2018). Moreover, they have already been used in the removal of some ECs, reaching efficiencies higher than 70%, which are comparable to other adsorbents. Banana peels have been used in the removal of atrazine (> 90%), ametrine (> 90%), sulfamethazole (70%), 17-ethinylestradiol (> 80%) and estrone (> 80%) (De Sousa et al., 2019). Therefore, the adsorptive removal of contaminants from wastewater could be an alternative of fruit peel valorization.

However, some peels have low adsorption capacity and separability from aqueous media. The adsorption capacity of peels will be enhanced with the impregnation of nanoparticles (iron oxides, titanium dioxide, zinc oxide, carbon nanotubes, among others), since nanoparticles have a greater specific surface area. The difficulties of separation between the adsorbent and the aqueous medium could be solved with the preparation of magnetically modified adsorbents. Magnetic separation is a fast, efficient and cost-effective method that can be used in both small-scale and large-scale wastewater treatment. Thus, magnetic composites with an agro-industrial residue matrix could be an alternative for the contaminant removal (Ahmed et al., 2020). Magnetite (Fe_3O_4) is an iron oxide commonly used in the adsorption of contaminants due to its magnetic character, low cost, environmentally friendly nature and the possibility of treating large volumes of wastewater. Magnetite has highly active surface sites and high surface area (between 30 and greater than 200 m^2/g), achieving adsorption capacities around 100 mg/g in the removal of ECs (Zheng et al., 2018, Ahmed et al., 2020). Magnetic composites (agro-industrial residues + magnetite) have been used in several studies with heavy metals and dyes (i.e. brilliant black, methylene blue), obtaining efficiencies between 90 and 99% (Zheng et al., 2018; Çatlıoğlu et al., 2020). Zheng et al. (Ahmed et al., 2020), reported that diclofenac was removed using a magnetic composite (MOF-100(Fe)) obtaining a removal efficiency of 80%.

Despite the efficiency obtained with magnetic adsorbents, only a few studies have been carried out to remove ECs. Therefore, the objective of this work was to evaluate if the caffeine removal from synthetic solutions improves when magnetic composites (fruits of high production in several countries around the world, and particularly in Ecuador) are used. For the study, the influence of the adsorbent dose, contact time and initial concentration of caffeine were evaluated, the obtained data were adjusted to different isotherm and kinetic models. Likewise, it was determined whether the presence of the magnetic particles facilitates the separation of the adsorbent from aqueous solutions.

2. Materials and methods

2.1. Material conditioning and composite synthesis

The orange peels were collected at the southern zone of Quito city (−0.266667; −78.5333), while the banana peels were donated by a company that processes the fruit in Ecuador. The iron salts used were $FeCl_3 \bullet 6H_2O$ and $FeSO_4 \bullet 7H_2O$ from Sigma Aldrich. Sodium hydroxide and all the other reagents used were at least 98.0% w/w pure.

Peels were cut and washed with drinking and distilled water to remove impurities. Then the peels were dried at 60 °C for 24 h, grinded in a knife mill (Thomas Wiley, model 3379-K05, Thomas Scientific) and sieved. The material between 125 and 149 μm was used in adsorption tests (Castro et al., 2021).

The co-precipitation method was used for the synthesis of magnetite. For this purpose, $FeCl_3 \bullet 6H_2O$ and $FeSO_4 \bullet 7H_2O$ were used, in a 3:2 M ratio. The mixture was heated to 70 °C with constant bubbling of argon and stirring at 1250 rpm. An 8.0 M NaOH solution was added to reach a pH 11. Then, the materials were separated from the aqueous solution by using a magnet. Magnetite was washed with distilled water to achieve pH 7.0 and dried at 80 °C for 12 h.

The synthesis of magnetic composites began with the procedure used for the synthesis of magnetite. Immediately after reaction with NaOH, 5.00 g of the previously conditioned peels were added to the magnetite solution. The mixture was kept under constant stirring at 70 °C for 30 min. The composite was magnetically separated, washed until pH= 7.0 and dried at 80 °C for 12 h (Castro et al., 2021; Kapur and Mondal, 2016).

2.2. Material characterization

The materials were characterized using ASTM standards to evaluate their physical chemical characteristics. Lignin, hemicellulose and cellulose (ASTM D1106–21); (ASTM D1109–21), extractives (ASTM D1107–21; ASTM D1110–21), moisture content (ASTM D 4442–20), ash (ASTM D 1102–21), volatile matter (ASTM E 872–19) and pH (D 4972–19) were determined.

The main functional groups of the synthesized adsorbents were identified by Raman and Fourier transform infrared spectroscopy (FT-IR). The Raman analyses were performed using a Horiba Scientific equipment, LabRam Evolution model, with a 532 nm wavelength laser, power of 50 mW at 5.0%, hole size of 180 and rate of 2.4. The FT-IR analyses were performed using a Perkin Elmer Spectrum 200 spectrometer within the 4000 - 500 cm^{-1} range.

The morphology of the adsorbents was studied using a Tescan Mira 3 equipped with a Schottky field emission gun at 20 kV. EDS was performed in a SEM chamber, using a detector Bruker X-Flash 6|30 with a 123 eV resolution. X-ray diffraction patterns were recorded in a Panalytical diffractometer model AERIS RESEARCH, using a copper X-ray tube (K_α, λ = 1.54056 Å) at 40 kV and 15 mA. The diffractogram analysis was performed on the average of four measurements between 5° and 85° (θ–2θ, Bragg-Brentano geometry) using the HighScore Plus software. The surface characteristics of the adsorbents (surface area, pore size and pore volume) were determined with BET analysis, using a 1LX micrometer NOVA touch. The adsorbents were conditioned under vacuum up to 100 °C with a heating rate of 10 °C/min, then they were held for 1440 min.

2.3. Batch adsorption tests

The batch adsorption tests were carried out to determine the dose of adsorbents and contact time that achieve the highest caffeine removal. Moreover, the influence of the initial concentration of caffeine was analyzed. The caffeine removal was evaluated using a 30 mg/L caffeine solution. In previous studies caffeine solutions between 5 and 5000 ppm

using crude (grape stalk) and modified/advanced/non-conventional adsorbents (activated carbons, nanoparticles and nanocomposites) were applied (Rigueto et al., 2020; Panneerselvam et al., 2011; I. Anastopoulos et al., 2020).

The process was carried out at room temperature (22.7 ± 1.0 °C), pH = 6.9 ± 0.24 and stirring at 150 rpm. The adsorbent material doses used were between 0.5 and 10.0 g/L. Eight tests were carried out for each adsorbent material with testing times between 5 and 180 min. Finally, to determine the influence of the initial caffeine concentration in the adsorption process, solutions between 10 and 50 mg/L were used. The batch tests were carried out in triplicate, using distilled water as control. After each experiment, the adsorbent was removed from the aqueous phase using magnetic separation and a 0.20 μm pore size filter membrane. Measurements of caffeine concentrations were performed in an Analytik Jena Specord 210 Plus UV - VIS spectrophotometer, at 287 nm.

2.4. Kinetic and isotherm study tests

Kinetic and isotherm studies were conducted at room temperature (22.7 ± 1.0 °C), pH = 6.9 ± 0.24 and stirring at 150 rpm using the optimal dose and contact time, respectively. In the adsorption kinetic tests, caffeine solutions of 30 mg/L and in the isothermal ones, caffeine concentrations between 10 and 90 mg/L were used. The pseudo first order (1), pseudo second order (2) and Elovich (3) kinetic models were fitted to the obtained data.

$$q_t = q_e\left(1 - e^{-k_1 * t}\right) \tag{1}$$

$$\frac{t}{q_t} = \frac{1}{k_2 * {q_e}^2} + \frac{t}{q_e} \tag{2}$$

$$q_t = \frac{1}{\beta} ln(1 + \alpha\beta t) \tag{3}$$

Moreover, to analyze the diffusion mechanism, the intraparticle diffusion model (4) was used to obtain information about the adsorption process.

$$q_t = k_p\sqrt{t} + C \tag{4}$$

where q_t is the amount of caffeine adsorbed at time t, (mg/g), q_e is the amount of caffeine adsorbed at equilibrium, (mg/g), k_1 is the first order kinetic constant, (min^{-1}), k_2 is the second kinetic constant order, (g/mg min), α is the initial rate constant, (mg/g min), β is the desorption constant (mg/g), k_p is the rate constant of the intra-particle diffusion model, (mg/g $min^{1/2}$) and C is a constant associated with the thickness of the boundary layer (mg/g).

On the other hand, the Langmuir, Freundlich and Sips isotherm models were used to determine the adsorption model that better fitted the results obtained. For this purpose, the non-linear equations showed in Equations 5 – 7 were used, respectively.

$$q_e = \frac{q_m * K_L * C_e}{1 + K_L * C_e} \tag{5}$$

$$q_e = K_F * {C_e}^{1/n} \tag{6}$$

$$q_e = \frac{q_m\left(K_L * C_e\right)^{1/n}}{1 + \left(K_L * C_e\right)^{1/n}} \tag{7}$$

where q_e is the equilibrium adsorption capacity (mg/g), q_m is the maximum adsorption capacity (mg/g), C_e is the concentration of caffeine at equilibrium (mg/L), K_L is the empirical constant of the Langmuir equation related to energy of adsorption (L/mg), K_F is the Freundlich constant (mg/g), and n is the adsorption intensity (I. Anastopoulos et al., 2020; Nguyen et al., 2021). The tests to determine the kinetics and isotherm model were carried out in triplicate.

Table 1
Physico-chemical characteristics of orange and banana peels.

Parameter	Orange peel (mean + SD)	Banana peel (mean + SD)
pH	5.2 ± 0.0	6.3 ± 0.0
Moisture (%)	65.0 ± 0.4	86.2 ± 0.3
Volatile material (%)	77.1 ± 0.1	69.8 ± 0.1
Ash (%)	8.2 ± 0.1	6.4 ± 0.3
Extractives (ethanol-toluene) (%)	18.4 ± 2.6	8.8 ± 1.7
Extractives (water) (%)	5.9 ± 0.5	4.7 ± 0.6
Total extractives (%)	24.3 ± 3.2	13.5 ± 2.3
Lignin (%)	23.1 ± 0.5	16.6 ± 1.1
Hemicellulose (%)	15.4 ± 0.3	15.9 ± 0.1
Cellulose (%)	33.3 ± 3.0	50.0 ± 1.0

2.5. Statistical analysis

The statistical analysis of data considered the calculation of means, standard deviations and linear regressions. The values were calculated using Microsoft Excel and its Solver tool (2013 version). The optimal contact time and adsorbent dose were determined using an analysis of variance (ANOVA) with a single factor analyzed by Tukey's test with a significance level of 95.0%. ANOVA analysis was performed using the Minitab 18 software 1.0 version.

In the non-linear kinetics and isotherm models, the coefficient of determination (R^2), the chi-square (χ^2) and the sum of squared errors (SSE) were calculated to determine the model that best fitted the caffeine adsorption data. The equations 8 - 10 were used to calculate the statistical parameters:

$$R^2 = 1 - \frac{\sum\left(q_{e,\,exp} - q_{e,\,cal}\right)^2}{\sum\left(q_{e,\,exp} - q_{e,\,mean}\right)^2} \tag{8}$$

$$\chi^2 = \sum \frac{\left(q_{e,\,exp} - q_{e,\,cal}\right)^2}{q_{e,\,cal}} \tag{9}$$

$$SSE = \sum\left(q_{e,\,exp} - q_{e,\,cal}\right)^2 \tag{10}$$

where $q_{e,exp}$ is the adsorption capacity of the adsorbents at equilibrium (mg/g), $q_{e,cal}$ is the adsorption capacity calculated using the Solver tool (mg/g) and $q_{e,mean}$ is the mean of $q_{e,exp}$ values (mg/g) (Nguyen et al., 2021).

3. Results and discussion

3.1. Physical-chemical characterization

Table 1 summarizes the physicochemical properties of the peels. The moisture is higher (21.2%) in the banana peel. Both peels have high volatile material contents (between 69.8 and 77.1%) due to their organic nature (lignin, cellulose, hemicellulose, lipid, protein and carbohydrate presence) (Kamsonlian et al., 2011). The total extractives content is higher in the orange peel (around 10%) than in the banana peel. This value represents the content of oils, fats and proteins, components that form bonds between the contaminant and the adsorbent and allow the efficient contaminant removal (Orozco et al., 2014).

Fruit peels have a low ash content, between 6.4 and 8.2%. Ash contents of 5.0% and 4.0% have been reported for banana and orange peels. Ash represents the inorganic matter that is formed by minerals (e.g. silica) and micronutrients. In high concentrations, the adsorption process could be affected due to ash low adsorption capacity (Pathak et al., 2017). The lignin (23.1 - 16.6%), cellulose (33.3 - 50.0%) and hemicellulose (15.4 - 15.9%) contents are higher in orange and banana peels compared to the other components, respectively. This is because agro-industrial residues are abundant in polysaccharides (cellulose and hemicelluloses) and lignin, which are part of the structure of the cell wall.

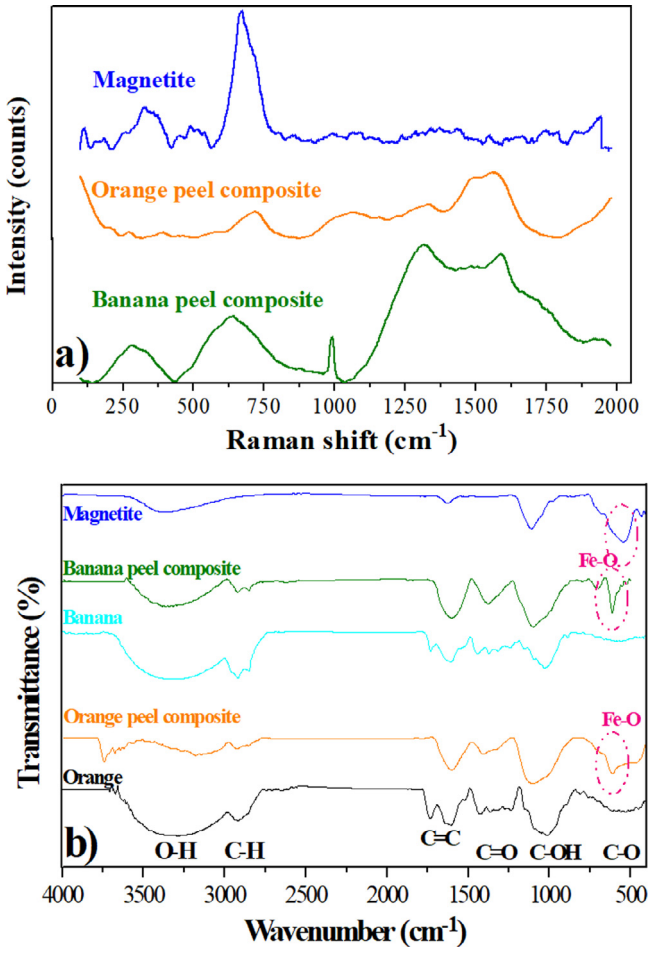

Fig. 1. a) Raman spectra and b) FT-IR spectra of adsorbent materials.

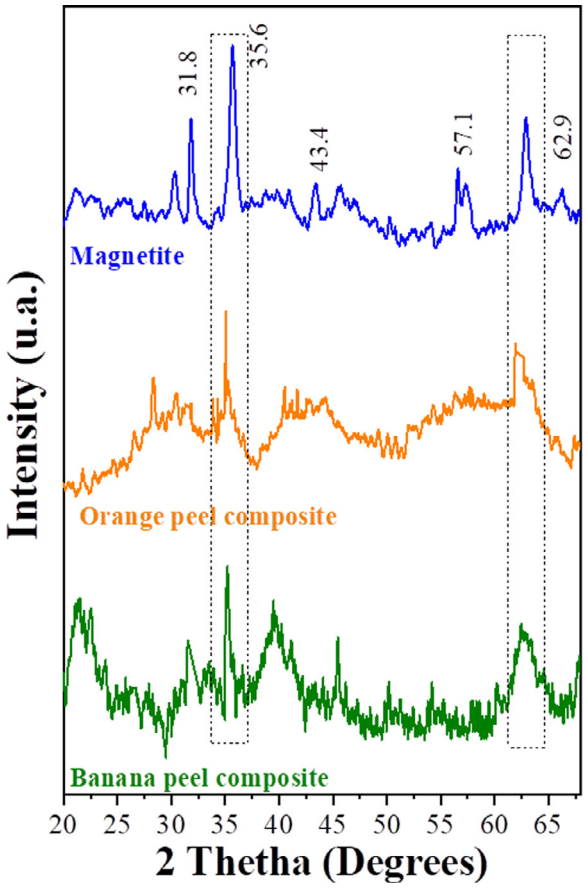

Fig. 2. XRD analysis of adsorbent materials.

Lignin, cellulose and hemicellulose indicate the presence of carboxyl, hydroxyl and other functional groups capable of interacting with contaminants. The high content of lignin, cellulose and hemicellulose suggests that orange and banana peels could be effective bio-adsorbents for the removal of organic contaminants (Almeida-Naranjo et al., 2021).

3.2. Instrumental characterization

Fig. 1a shows Raman spectra for magnetic composites. They show the presence of magnetite bands (319.20, 535.98 and 668.33 cm^{-1} on magnetite, 638.13 cm^{-1} on the orange peel composite and 619.40 cm^{-1} on the banana peel composite). Additionally, there are other bands belonging to maghemite, formed by the oxidation of magnetite (around 350, 500 and 700 cm^{-1}). Therefore, the magnetic composites and the magnetite particles exhibit a mixture of magnetite and maghemite. The additional peaks in the composites are attributed to the nature of peels (Shebanova and Lazor, 2003).

Fig. 1b shows the infrared spectra for orange and banana peels. They present intense peaks at 3281.3 and 3321.8 cm^{-1}, for orange and banana peels respectively, the bands are characteristic of hydroxyl groups (O–H). The peaks at 2917.8 cm^{-1} (orange peel), 2918.7 and 2851.2 cm^{-1} (banana peel) correspond to the C–H vibrations of the stretch methyl (CH_3), methylene (CH_2) and methoxy groups (O–CH_3), main components of lignin and pectin. The peaks around 1730 cm^{-1} are characteristic of the carbonyl group (C = O) stretch, they represent the presence of aldehydes, ketones and the carbonyl ester group. The peaks around 1600.0 cm^{-1} represent the C = C bond stretch and could show the presence of benzene, aromatic rings, or amino acids. At 1422.2 cm^{-1} and 1442.5 cm^{-1} (orange and banana peel, respectively) is observed the presence of aliphatic, aromatic groups, vibrations of methyl, methylene and methoxy groups resulting from the vibration of the aromatic ring of lignin (Feng et al., 2009). The bands around 1000.0 cm^{-1} represent the C–O group from alcohols, phenols and carboxylic acids and represents the band of hemicellulose, cellulose and lignin. Finally, the band in the region of 500.0 cm^{-1} was attributed to the presence of amino groups (Alaa El-Din et al., 2018; Dahiru et al., 2018).

In the magnetite, there were bands around 3371.9 cm^{-1}, typical of hydroxyl groups. The band around 1624.7 cm^{-1} corresponds to the vibration of the carboxylate and amide groups. At 1110.8 cm^{-1} the stretching vibration of C–OH and C–O was presented. The intense peak at 547.7 cm^{-1} is related to the stretching vibration of Fe-O (iron oxides), evidencing the magnetic particle presence (Gupta and Nayak, 2012).

The FT-IR spectra for the composites show that the peaks of the functional groups from peels are maintained. However, the hydroxyl and C–H groups have reduced their intensity due to the reactions generated in the magnetite impregnation process. The peak of the carbonyl group decreases in the spectral images. The peaks at 611.32 and 552.51 cm^{-1}, for the orange peel and banana peel composites, respectively; evidence the presence of iron oxides in the materials (Kapur and Mondal, 2016; Dahiru et al., 2018). The presence of the functional groups in lignin, cellulose, hemicellulose and in the iron oxides indicate that the materials studied could be good adsorbents.

The XRD patterns of magnetite and the composites are shown in Fig. 2. Magnetite (peaks at 2θ = 31.8, 35.6 and 62.9°) and maghemite (peaks at 2θ = 35.6, 43.4 and 57.1°) were identified. In the composites, the most intense bands of magnetite (peaks at 2θ = 35.6 and 62.9°) were observed (Liu et al., 2014).

Table 2 shows the parameters of BET analysis for the adsorbents. The specific surface area of orange and banana peels is small (0.8 and 0.08, respectively). The obtained results coincide with those reported by previous studies (orange: 0.83 m^2/g and banana: < 0.1 m^2/g) (Liu et al., 2014; Stavrinou et al., 2018; Feng and Guo, 2012). The low values of surface area and pore volume are attributed to the presence of pectin, lignin and viscous compounds that the fruit peels present. This is verified by what is observed in Fig. S1. Despite the heterogeneous surface, it is observed that the particles are compact mainly in banana (Fig. S1b), leaving very little spaces (pores) between them. Heterogeneous surfaces favor the adsorption process (Oyekanmi et al., 2019).

As can be observed in Fig. S1, the surface of the composites showed the presence of smaller particles of different sizes distributed randomly on the fruit peels, due to the inclusion of magnetite nanoparticles (57.3 m^2/g). As a result, the composites increased their surface area and pore volume, as suggested by Ahmed et al. (Ahmed et al., 2020) and Çatlıoğlu et al. (Zheng et al., 2018; Çatlıoğlu et al., 2020). Panneerselvam et al. (Panneerselvam et al., 2011), also showed an increase in the surface area of tea waste when impregnating it with magnetite nanoparticles. The presence of Fe in both composites was confirmed with EDS graph with the peak at 6.4 keV (Figs. S1d and S1f). On the other hand, the N_2 adsorption - desorption isotherms of the materials are type II, according to the IUPAC classification. This is characteristic of non-porous or microporous materials (Çatlıoğlu et al., 2021).

3.3. Adsorption process

The material dose used for the caffeine removal is showed in Fig. 3a. An increase in the dose of fruit peels and composites produces a higher efficiency, due to the greater surface area and functional groups present (Ahmed et al., 2020). The highest caffeine removal efficiencies (mean + SD) achieved with orange and banana peels were 95.5 ± 0.3% and 90.5 ± 0.5%, using 3.5 g/L and 9.5 g/L, respectively. The higher dose of banana peels required could be due to their lower lignin contents in their composition (around 7.0% less) compared to orange peels. A higher lignin content in the orange peel suggests the formation of bonds between the hydroxyl and carboxyl functional groups and caffeine, process by which caffeine was efficiently removed (Almeida-Naranjo et al., 2021).

The carbonyl group, C = C group and C–O group present in the orange peel have a higher intensity than those of the banana peel. In addition, the SEM images for the peels show different morphologies, the orange peels are the ones that present higher porosity. This is characteristic of agro-industrial residues, and favors the retention of caffeine (Liu et al., 2016).

Fig. 3a shows that magnetite (using a dose of 5 g/L) reached a maximum caffeine removal of 41.3 ± 0.5%, after 3 h of contact time. In the caffeine removal, electrostatic interaction occurs by H-bond interaction (hydrogen bridges) and the π-π interaction. In some carbonaceous materials, the carbon surface has polar groups with hydrophilic behavior, such as –NH, –OH, –O and –COO. Consequently, caffeine adsorption could occur by dipole-dipole interactions (Rigueto et al., 2020). However, the agglomerates and non-homogeneous size distribution formed during magnetite synthesis (showed in SEM images) produce a reduction of active sites in its surface (Zheng et al., 2018). The composites improved the caffeine removal (9.0% for orange peels and 23.0% for banana peels). In this case, 2.5 g/L of magnetic orange peel and 5.5 g/L of magnetic banana peel removed 93.6 ± 0.2% and 89.2 ± 0.01%, respectively; after 3 h of contact time. An improvement in the removal percentage using composites has been also reported by Edathil et al. (Edathil et al., 2018) when coffee waste was used as a matrix to synthesize a magnetic coffee waste by dispersing Fe_3O_4 nanoparticles on its surface via a single pot precipitation method in order to remove Pb^{+2} from aqueous solutions (18% compared with waste without modification).

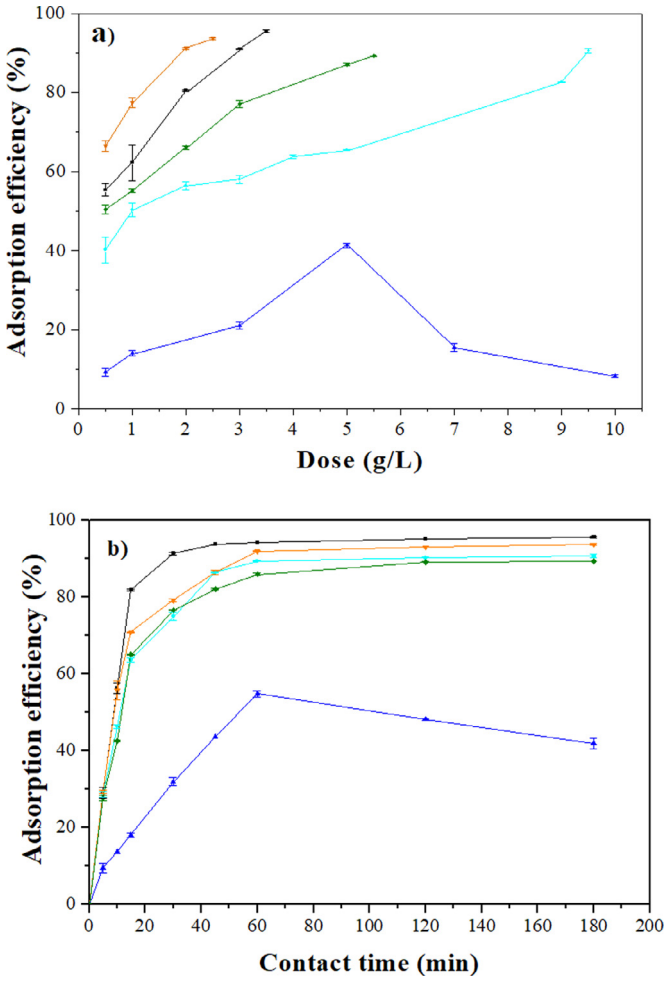

Fig. 3. Optimal conditions for caffeine removal: a) optimal dose, b) optimal contact time. Black line: orange peel, cyan line: banana peel, blue line: magnetite, orange line: orange peel composite, green line: banana peel composite.

The use of the 8.0 M NaOH solution generated the degradation of the peel's components due to the demethylation of the methyl ester present in lignin, cellulose and hemicellulose. In the FT-IR spectra (Fig. 1b) the demethylation process is observed in the changes that the composites present compared to the fruit peels, showing a decrease in the intensity of the bands around 1750 cm^{-1} and an increase in the intensity of the bands around 1000 and 1640 cm^{-1}. The amount of the carboxylate ion increases on the peel surface during this process (Kapur and Mondal, 2016; Stavrinou et al., 2018). According to Feng and Guo (Feng et al., 2010), the carboxyl groups are responsible for the binding between adsorbent and the adsorbate, increasing the adsorption capacity of caffeine. Furthermore, the presence of NaOH causes the swelling of lignocellulosic compounds, which increases the surface area and reduces both the degree of polymerization and the crystallinity of the fruit peels, thus it favors their adsorption capacity (Sharma et al., 2018). The caffeine removal using the composites is higher than the one obtained by using only magnetite (caffeine removal around 50%), as observed in previous similar studies (Medina-Espinosa et al., 2021). This seems to be influenced by the change that the fruit peels have undergone in the magnetite co-precipitation process. Additionally, separating the composites from the aqueous solution after the adsorption process was easier than removing the fruit peels (Fig. S2).

Fig. 3b shows the removal as a function of contact time using the optimal dose of each material. The fruit peels and their composites showed rapid adsorption during the first 10 min, then the adsorption gradually

Table 2
Surface area, pore volume and pore diameter of adsorbents.

Adsorbents	Surface area (m^2/g)	Pore volume*10^{-3} (cm^3/g)	Pore diameter (nm)	N_2 adsorption/desorption isotherm Volume adsorbed/desorbed (cm^3/g STP) vs Relative pressure (P/P_o) Black line: Adsorption isotherm Orange line: Desorption isotherm
Orange peel	0.801	2.560	3.9906	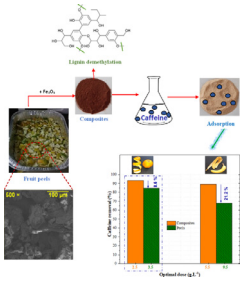
Banana peel	0.079	0.452	7.078	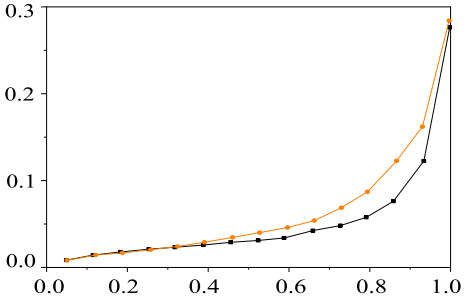
Magnetite	57.258	592.206	12.102	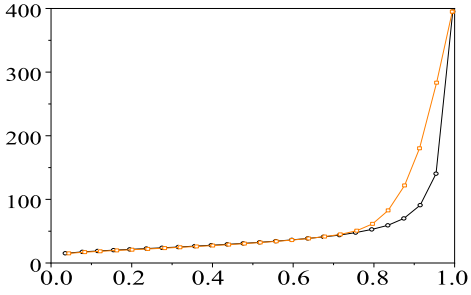
Orange peel composite	14.282	62.814	13.255	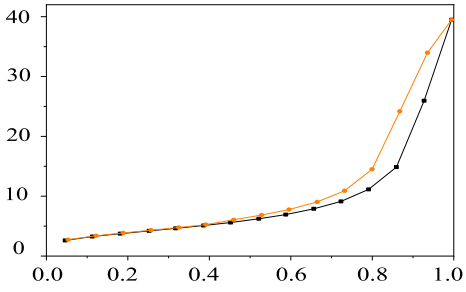
Banana peel composite	8.140	32.420	3.440	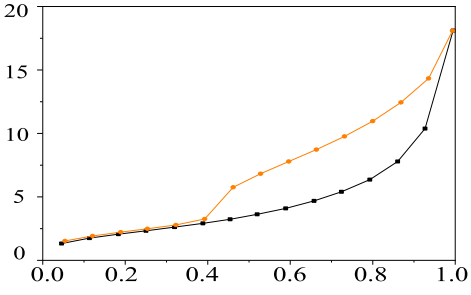

Table 3
Kinetic parameters calculated from pseudo first order, pseudo second order and Elovich models for the adsorption of caffeine.

			Adsorbents				
Kinetic model	Parameter	Unit	Orange peel	Banana peel	Magnetite	Orange peel composite	Banana peel composite
Experimental data	q_e	mg/g	8.889	3.088	3.091	12.174	5.269
Pseudo first order	q_e	mg/g	8.977	3.072	3.118	11.972	5.056
	K_1	1/min	0.095	0.074	0.034	0.089	0.112
	R^2	–	0.985	0.994	0.997	0.991	0.981
	χ^2	–	0.179	0.009	0.005	0.192	0.062
	SSE	–	1.249	0.046	1.571	10.474	12.006
Pseudo second order	q_e	mg/g	9.918	3.445	3.695	13.328	5.518
	K_2	g/(mg min)	0.013	0.028	0.010	0.009	0.030
	R^2	–	0.956	0.987	0.991	0.984	0.998
	χ^2	–	0.539	0.017	0.017	0.333	0.005
	SSE	–	3.279	0.093	1.567	8.078	10.346
Elovich	A	mg/(g min)	5.437	1.416	0.227	5.696	6.483
	β	mg/g	0.635	1.788	1.158	0.452	1.286
	R^2	–	0.887	0.952	0.974	0.936	0.976
	χ^2	–	0.868	0.015	0.048	0.625	0.008
	SSE	–	7.926	0.485	1.566	11.529	10.345

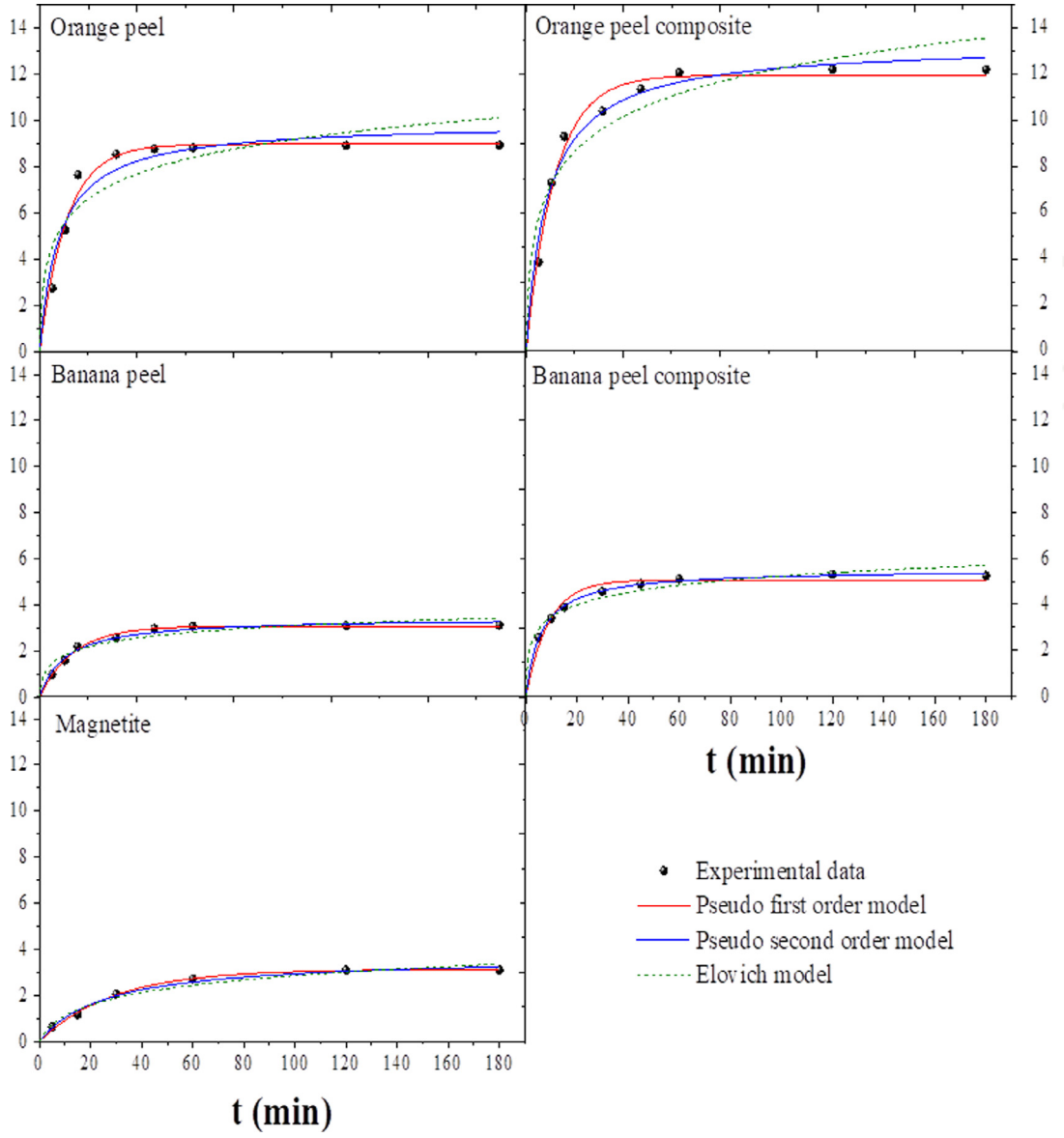

Fig. 4. Pseudo first order, pseudo second order and Elovich kinetic models for adsorption of caffeine.

Table 4
Isotherm parameters calculated from Langmuir, Freundlich and Sips models.

			Adsorbents				
Isotherm model	Parameter	Unit	Orange peel	Banana peel	Magnetite	Orange peel composite	Banana peel composite
Langmuir	q_m	mg/g	15.188	6.761	4.905	25.604	11.668
	K_L	L/mg	0.978	0.310	0.049	0.412	0.238
	R^2	–	0.978	0.981	0.927	0.999	0.993
	χ^2	–	0.028	0.008	0.016	0.002	0.005
	SSE	–	1.154	0.126	0.183	0.091	0.121
Freundlich	K_F	$(mg/g)^{1-1/n}$	7.152	1.679	0.465	7.636	2.569
	1/n	–	0.394	0.558	0.539	0.522	0.541
	R^2	–	0.966	0.970	0.876	0.987	0.972
	χ^2	–	0.042	0.013	0.027	0.022	0.020
	SSE	–	1.760	0.1971	0.309	1.332	0.519
Sips	q_m	mg/g	16.085	6.590	3.259	26.992	8.500
	K_L	L/mg	0.896	0.326	0.095	0.366	0.400
	n	–	1.211	0.979	0.509	1.052	0.650
	R^2	–	0.980	0.981	0.968	0.999	0.973
	χ^2	–	0.025	0.009	0.007	0.001	0.020
	SSE	–	1.036	0.126	0.079	0.072	0.502

Table 5
Results of caffeine removal onto different adsorbents.

Material	Specific area (m^2/g)	Dose (mg/L)	pH	Q_{max} (mg/g)	Isotherm model	Reference
Commercial PAC	882.6	3000	6.2	51.8	Freundlich	Toniciolli Rigueto et al., 2020
Composite from coffee residues and chitosan	–	200	6.0	8.66	Freundlich	
Charcoal from rice husk	63	1000	5.0	2.09	Langmuir	
Charcoal from rice husk blended with corn cob	144	1000	5.0	8.04	Langmuir	
Graphene	570.2	50	7.5	22.73	Langmuir	
Acacia mangium wood (activated carbon)	–	3000	7.7	30.3	–	Danish et al., 2020
Pineappple plan leaves (activated carbon)	1031	25	7	155.5	Langmuir	Beltrame et al., 2018
Babassu coco (activated carbon)	980	10	3	186.9	Langmuir	Couto et al., 2015
Tea leaves	–	–	–	435	Langmuir, Freundlich	Shider and Sidhu 2007
Raw grape stalk	–	–	–	89.194	Sips	Portinho et al., 2017
Grape stalk modified by phosphoric	–	–	–	129.568	Sips	
Activated carbon from grape stalk	1099.86	–	4	916.7	Sips	
Coconut waste (activated carbon)	–	–	–	171.23	Langmuir	Souza et al., 2017
Peach stones (helium, activated carbon)	1064	120	4.8	260	Sips	Torrellas et al., 2015
Peaches stones (activated carbon)	1216	120	6.3	260	Sips	
Peaches stones modified by oxidation (activated carbon)	959	120	6.3	270	Sips	

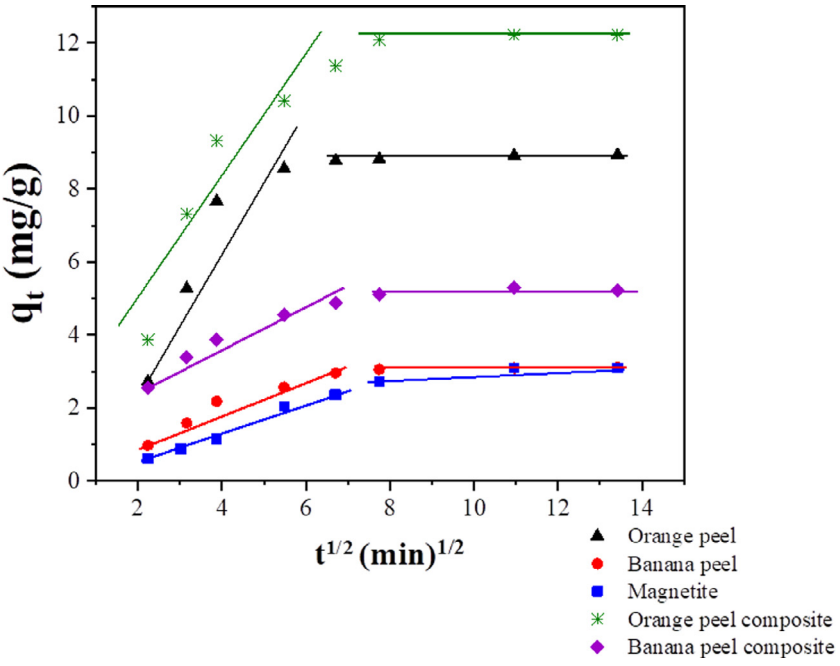

Fig. 5. Intraparticle diffusion kinetics for adsorption of caffeine.

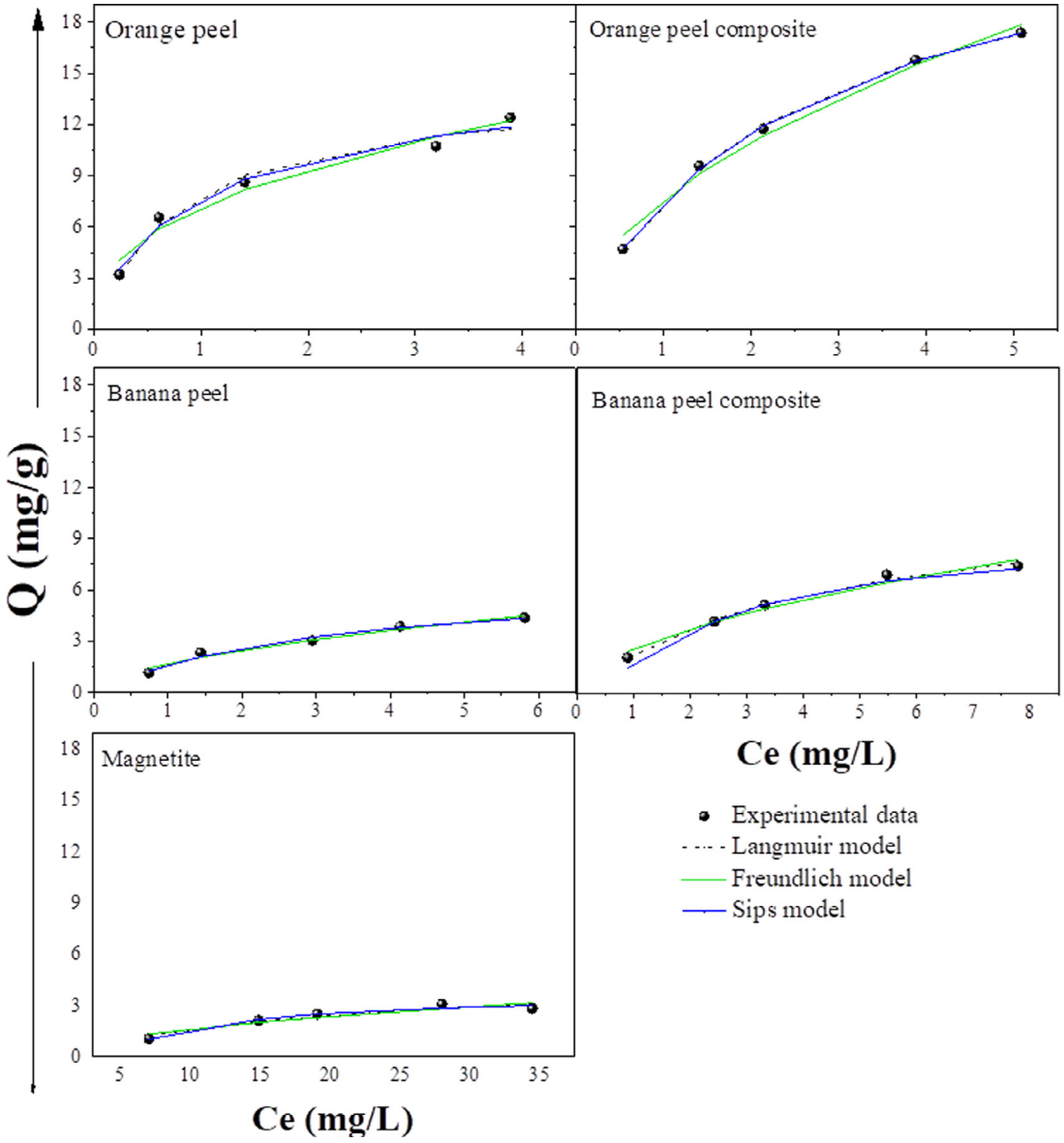

Fig. 6. Langmuir, Freundlich and Sips isotherm models for adsorption of caffeine.

slows down until equilibrium is reached. Banana peel, magnetite and composites reached concentrations close to the equilibrium (optimum contact time) at 60 min, while the orange peel achieved the equilibrium in 45 min. The maximum removals were 93.7 ± 0.06, 89.3 ± 0.1, 91.9 ± 0.1 and 85.9 ± 0.4% for orange peel, banana peel, orange peel composite and banana peel composite, respectively.

Adsorption on magnetite is slower, and the maximum caffeine removal was 54.8 ± 0.8% with a dose of 5 g/L in 60 min. Once the maximum electrostatic interaction is reached, the process efficiency decreases. Probably, this occurs due to the low magnetic intensity of the magnetite particles due to the formation of agglomerates, which are not of nanometric dimensions. Previous researchers have found that often the relative adsorption efficiency decreases because of particle aggregation/agglomeration that leads to a reduction of the specific surface area. Agglomeration/aggregation could become an obstacle between the caffeine molecules and the empty sites of the adsorbents (De Sousa et al., 2019; Panneerselvam et al., 2011).

On the other hand, it was determined that an increase in the initial caffeine concentration (from 10 to 50 mg/L) reduced the removal efficiency. This reduction was 6.1, 5.8, 13.7, 6.5 and 9.1% for orange peel, banana peel, magnetite, orange peel composite and banana peel composite, respectively. The decrease in the caffeine adsorption is produced by the presence of a greater quantity of caffeine molecules that are competing for the active sites available in the adsorbents (Bachmann et al., 2021).

3.4. Kinetic model

The adsorption kinetics determines the residence time required to complete the adsorption process. The pseudo first order, pseudo second order and Elovich models performed well (SSE= 0.007–73.532 and χ^2= 0.005–0.868) with R^2 values ranging from 0.887 to 0.994 for fruit peels, from 0.974 to 0.997 for magnetite, and from 0.936 to 0.998 for composites. The parameters and fittings for the different adsorption kinetics models considered are shown in Table 3 and Fig. 4.

Peels, magnetite and the orange composite adsorptions were best adjusted to the pseudo first order model while the banana composite adsorption was best adjusted to the pseudo second order kinetic model. However, the q_e value obtained using the pseudo-first order model is

closer to the experimental q_e value, as with the other 4 adsorbents. Although the pseudo-first order model adequately describes the adsorption kinetics of the experimental data for all adsorbents, this model does not reveal the adsorption mechanisms.

Generally, a solid-liquid adsorption process is characterized by a diffusion process, so it will be necessary to analyze this model (Tran et al., 2017). If the intraparticle diffusion curve passes through the origin, then intraparticle diffusion is the only one that limits the adsorption rate. However, Fig. 5 and table S1 show the presence of two linear regions, so the adsorption process is controlled by a multi-step mechanism. At first, there were a rapid diffusion of caffeine on the external surface of the adsorbents and later an intraparticle diffusion occurs. In the latter, the caffeine molecules migrate from the outside of the adsorbents into their pores, where the adsorption took place (Liu et al., 2014).

3.5. Adsorption isotherms

The contaminant distribution between the liquid phase and the adsorbent at equilibrium is determined by the adsorption isotherms. The Langmuir, Freundlich and Sips models were used to determine the caffeine distribution in the adsorbents; the data are presented in Table 4 and Fig. 6. Langmuir's model assumes that the adsorbent has active sites with the same energy (homogeneous surface) and caffeine adsorption occurs in a monolayer without lateral interaction. Freundlich's model assumes that active sites have different energies (heterogeneous surface) and that adsorption occurs in multilayers. Meanwhile, the Sips model is a combination between the Langmuir and Freundlich models (Sahoo and Prelot, 2020).

The studied materials have a higher correlation factor with the Langmuir and Sips isothermal models with values of correlation coefficients (R^2) between 0.927 and 0.999. A similar result was obtained by N'diaye & Ahmed Kankou (N'diaye and Ahmed Kankou, 2019) using *Ziziphus Mauritiana* seeds in the caffeine removal. K_L (Langmuir) and 1/n (Freundlich) values are < 1, so the caffeine adsorption is favorable in the adsorbents (Nguyen et al., 2021). Furthermore, lower values of SSE (0.079–1.76) and χ^2 (0.001–0.040) were achieved for the three models, being slightly higher for the Freundlich model. Likewise, the adsorption capacity values obtained from the Langmuir and Sips models are close to the values of the experimental adsorption capacity. Therefore, the results suggest that the caffeine adsorption take place onto a homogenous surface (I. Anastopoulos et al., 2020; Sharma et al., 2018; Medina-Espinosa et al., 2021).

Besharati & Alizadeh (Besharati and Alizadeh, 2018) showed strong positive evidence that the adsorption of malachite green dye onto lignocellulosic adsorbents impregnated with magnetite nanoparticles (tea waste, peanut husk, Azolla and fig leaves) follows the Langmuir isotherm, as well as the caffeine adsorption onto magnetite impregnated on used black tea (Mahmood et al., 2018). Moreover, the crystal violet dye adsorption on magnetized orange peels also exhibits a reasonable fit to the Langmuir model (Ahmed et al., 2020). Stavrinou et al. (Stavrinou et al., 2018) demonstrated that the Langmuir isotherm was found to describe satisfactorily the biosorption of methylene blue and orange G onto banana peels. In addition, the adsorption of rhodamine B using acid modified banana peels showed the same behavior. In addition, Beltrame et al. (K.K. Beltrame et al., 2018), showed that the adsorption of caffeine onto the surface of the prepared activated carbon fibers from pineapple plant leaves was fitted to the Langmuir isotherm model. In this work, the material with the highest adsorption capacity was the orange peel-magnetite composite (q_{max} = 25.6 mg/g), while the material with the lowest adsorption capacity was magnetite (q_{max} = 3.3 mg/g).

Table 5 lists some results for caffeine adsorptive removal from aqueous solutions with different adsorbents. Values of specific area, dose, pH, q_{max} and the isotherm model fitted are showed. Several adsorbents used in caffeine removal have a higher adsorption capacity than fruit peels and composites. This is linked to the high surface area of these adsorbents. However, most of these adsorbents are activated carbons, whose cost is higher than that of fruit peels and even composites. This cost is not analyzed in any of the previous studies. On the other hand, there are materials with adsorption capacities that are comparable to those of the materials studied in this work. Despite the high surface area of graphene and its relatively complex synthesis, its adsorption capacity is comparable to that of the orange peel composite. While the composite coffee residues + chitosan, charcoal from rice husk and charcoal from rice husk + corn cob present adsorption capacities similar to those obtained with fruit peels, magnetite and the banana peel composite (Besharati and Alizadeh, 2018; K.K. Beltrame et al., 2018; K.K. Beltrame et al., 2018; Danish et al., 2020; Couto et al., 2015).

4. Conclusions

The performance in the adsorption process improved with the use of the composites due to the chemical modification with sodium hydroxide (demethylation) and the larger magnetite surface area. The demethylation increases the number of carboxylate ligands on the composite surfaces allowing the caffeine removal from synthetic wastewater. Using 2.5 g/L of orange peel composite and 5.5 g/L of banana peel composite, an 8.6% and 21.2% higher efficiency in the caffeine removal was achieved compared to the non-modified orange and banana peels, respectively. The adsorption using the materials proposed fitted well to the Langmuir and Sips isotherm models, achieving removal capacities between 4.9 and 25.6 mg/g. On the other hand, the fruit peels, magnetite and composite adsorptions were adjusted to the pseudo first order kinetic model, while the adsorption process is controlled by a multi-step mechanism. Considering that the nanoparticle presence favors the removal of contaminants such as caffeine, the challenge for future work is to synthesize nanoparticulated magnetite and achieve a homogeneous distribution on fruit peels or other types of residues during impregnation.

Declaration of Competing Interests

The authors declare that they have no known competing financial interests or personal relationships that could have appeared to influence the work reported in this paper.

Acknowledgments

The authors would like to acknowledge the support of the Escuela Politécnica Nacional through the research project PIS-18-01. Authors want to pay a fair tribute with our work, to all the people who have suffered and died from COVID-19, in addition to the medical staff, for their work and dedication in these difficult times.

Supplementary materials

Supplementary material associated with this article can be found, in the online version, at doi:10.1016/j.envc.2021.100343.

References

Álvarez-Torrellas, S., Rodríguez, A., Ovejero, G., Gómez, J.M., García, J., 2016. Removal of caffeine from pharmaceutical wastewater by adsorption: influence of NOM, textural and chemical properties of the adsorbent. Environ. Technol. (United Kingdom) 37 (13), 1618–1630. doi:10.1080/09593330.2015.1122666.

Ahmed, M., Mashkoor, F., Nasar, A., 2020. Development, characterization, and utilization of magnetized orange peel waste as a novel adsorbent for the confiscation of crystal violet dye from aqueous solution. Groundw. Sustain. Dev., 100322 doi:10.1016/j.gsd.2019.100322.

Almeida-Naranjo, C.E., Frutos, M., Tejedor, J., Cuestas, J., Valenzuela, F., Rivadeneira, M.I., Villamar, C.A., Guerrero, V.H., et al., 2021. Caffeine adsorptive performance and compatibility characteristics (Eisenia foetida Savigny) of agro-industrial residues potentially suitable for vermifilter beds. Sci. Total Environ. 801, 149666. doi:10.1016/j.scitotenv.2021.149666.

Anastopoulos, I., et al., 2020a. Removal of caffeine, nicotine and amoxicillin from (waste) waters by various adsorbents. A review. J. Environ. Manage. 261. doi:10.1016/j.jenvman.2020.110236, no. January.

Anastopoulos, I., Katsouromalli, A., Pashalidis, I., 2020b. Oxidized biochar obtained from pine needles as a novel adsorbent to remove caffeine from aqueous solutions. J. Mol. Liq. 304, 112661. doi:10.1016/j.molliq.2020.112661.

Bachmann, S.A.L., Calvete, T., Féris, L.A., 2021. Caffeine removal from aqueous media by adsorption: an overview of adsorbents evolution and the kinetic, equilibrium and thermodynamic studies. Sci. Total Environ. 767, 144229. doi:10.1016/j.scitotenv.2020.144229.

Beltrame, K.K., Cazetta, A.L., de Souza, P.S.C., Spessato, L., Silva, T.L., Almeida, V.C., 2018a. Adsorption of caffeine on mesoporous activated carbon fibers prepared from pineapple plant leaves. Ecotoxicol. Environ. Saf. 147, 64–71. doi:10.1016/j.ecoenv.2017.08.034, no. August 2017.

Beltrame, K.K., Cazetta, A.L., De Souza, P.S.C., Spessato, L., Silva, T.L., Almeida, V.C., 2018b. Ecotoxicology and environmental safety adsorption of caffeine on mesoporous activated carbon fibers prepared from pineapple plant leaves. Ecotoxicol. Environ. Saf. 147, 64–71. doi:10.1016/j.ecoenv.2017.08.034, no. August 2017.

Besharati, N., Alizadeh, N., 2018. Adsorption of malachite green dye on different natural absorbents modified with magnetite nanoparticles. J. Nanoanalysis 5 (3), 143–155. doi:10.22034/jna.2018.551649.1048.

Boretti, A., Rosa, L., 2019. Reassessing the projections of the world water development report. npj Clean Water doi:10.1038/s41545-019-0039-9, no. June.

Castro, D., Rosas-Laverde, N.M., Aldás, M.B., Almeida-Naranjo, C.E., Guerrero, V.H., Pruna, A.I., Apr. 2021. Chemical modification of agro-industrial waste-based bioadsorbents for enhanced removal of Zn(II) ions from aqueous solutions. Materials (Basel) 14 (9), 2134. doi:10.3390/ma14092134.

Çatlıoğlu, F.N., et al., 2020. Fe-modified hydrochar from orange peel as adsorbent of food colorant Brilliant Black: process optimization and kinetic studies. Int. J. Environ. Sci. Technol. 17 (4), 1975–1990. doi:10.1007/s13762-019-02593-z.

Çatlıoğlu, F., et al., 2021. Preparation and application of Fe-modified banana peel in the adsorption of methylene blue: process optimization using response surface methodology. Environ. Nanotechnology, Monit. Manag. 16. doi:10.1016/j.enmm.2021.100517, no. April.

Couto, O.M., Matos, I., da Fonseca, I.M., Arroyo, P.A., da Silva, E.A., de Barros, M.A.S.D., 2015. Effect of solution pH and influence of water hardness on caffeine adsorption onto activated carbons. Can. J. Chem. Eng. 93 (1), 68–77. doi:10.1002/cjce.22104.

Dahiru, M., Zango, Z.U., Haruna, M.A., 2018. Cationic dyes removal using low-cost banana peel biosorbent. Am. J. Mater. Sci. 8 (2), 32–38. doi:10.5923/j.materials.20180802.02.

Danish, M., Birnbach, J., Mohamad Ibrahim, M.N., Hashim, R., 2020. Scavenging of caffeine from aqueous medium through optimized H3PO4-activated Acacia mangium wood activated carbon: statistical data of optimization. Data Br 28, 105045. doi:10.1016/j.dib.2019.105045.

De Sousa, P.A.R., et al., 2019. Evaluation of the adsorption capacity of banana peel in the removal of emerging contaminants present in aqueous media - Study based on factorial design. Braz. J. Anal. Chem. 6 (22), 14–28. doi:10.30744/brjac.2179-3425.AR.119-2018.

Edathil, A.A., Shittu, I., Zain, J.H., Banat, F., Haija, M.A., 2018. Novel magnetic coffee waste nanocomposite as effective bioadsorbent for Pb(II) removal from aqueous solutions. Environ. Chem. Eng. doi:10.1016/j.jece.2018.03.041, no. Ii.

Feng, N.C., Guo, X.Y., 2012. Characterization of adsorptive capacity and mechanisms on adsorption of copper, lead and zinc by modified orange peel. Trans. Nonferrous Met. Soc. China (English Ed. 22 (5), 1224–1231. doi:10.1016/S1003-6326(11)61309-5.

Feng, N.C., Guo, X.Y., Liang, S., 2010. Enhanced Cu(II) adsorption by orange peel modified with sodium hydroxide. Trans. Nonferrous Met. Soc. China (English Ed. 20, s146–s152. doi:10.1016/S1003-6326(10)60030-1, no. SUPPL.1.

Gupta, V.K., Nayak, A., 2012. Cadmium removal and recovery from aqueous solutions by novel adsorbents prepared from orange peel and Fe2O3 nanoparticles. Chem. Eng. J. 180, 81–90. doi:10.1016/j.cej.2011.11.006.

Kamsonlian, S., Suresh, S., Majumder, C.B., Chand, S., 2011. Characterization of banana and orange peels : biosorption mechanism. Int. J. Sci. Technol. Manag. 2 (4), 1–7.

Kapur, M., Mondal, M.K., 2016. Magnetized sawdust for removal of Cu (II) and Ni (II) from aqueous solutions. Desalin. Water Treat. 57 (27), 12620–12631. doi:10.1080/19443994.2015.1049962.

Korekar, C., Kumar, G., Ugale, A., 2019. Occurrence, fate, persistence and remediation of caffeine: a review. Environ. Sci. Pollut. Res. doi:10.1007/s11356-019-06998-8.

Kot-Wasik, A., Jakimska, A., Śliwka-Kaszyńska, M., 2016. Occurrence and seasonal variations of 25 pharmaceutical residues in wastewater and drinking water treatment plants. Environ. Monit. Assess. 188 (12). doi:10.1007/s10661-016-5637-0.

Liu, Y., Zhu, X., Qian, F., Zhang, S., Chen, J., 2014. Magnetic activated carbon prepared from rice straw-derived hydrochar for triclosan removal. RSC Adv 4 (109), 63620–63626. doi:10.1039/c4ra11815d.

Liu, J., Li, E., You, X., Hu, C., and Huang, Q. “Adsorption of methylene blue on an agro-waste oiltea shell with and without fungal treatment,” no. November, pp. 1–11, 2016, doi: 10.1038/srep38450.

Long, J., et al., 2019. Inactive Fusarium Fungal strains (ZSY and MJY) isolation and application for the removal of Pb(II) ions from aqueous environment. J. Ind. Eng. Chem. 72, 442–452. doi:10.1016/j.jiec.2018.12.047, no. Ii.

Mahmood, T., Aslam, M., Naeem, A., Ali, R., 2018. Equilibrium, kinetics, mechanism and thermodynamics studies of As (III) adsorption from aqueous solution using iron impregnated used tea Equilibrium, kinetics, mechanism and thermodynamics studies of As (III) adsorption from aqueous solution using. Desalin. Water Treat. doi:10.5004/dwt.2018.21855, no. January.

Martínez-Ruano, J.A., Caballero-Galván, A.S., Restrepo-Serna, D.L., Cardona, C.A., 2018. Techno-economic and environmental assessment of biogas production from banana peel (Musa paradisiaca) in a biorefinery concept. Environ. Sci. Pollut. Res. 25 (36), 35971–35980. doi:10.1007/s11356-018-1848-y.

Medina-Espinosa, T., Asimbaya, C.G., Galeas, S., Rosas-Laverde, N., Debut, A., Guerrero, V.H., 2021. Adsorptive removal of chromium (VI) from synthetic waters using magnetic lignocellulosic composites. IOP Conf. Ser. Earth Environ. Sci. In press.

N’diaye, D.A., Ahmed Kankou, M.S., 2019. Sorption of caffeine onto low-cost sorbent : application of two and three-parameter isotherm models. Appl. J. Environ. Eng. Sci. 3, 263–272. doi:10.48422/IMIST.PRSM/ajees-v5i3.17210.

Nguyen, L.H., et al., 2021. Paper waste sludge-derived hydrochar modified by iron (III) chloride for enhancement of ammonium adsorption: an adsorption mechanism study. Environ. Technol. Innov. 21, 101223. doi:10.1016/j.eti.2020.101223, no. Iii.

Orozco, R.S., et al., 2014. Characterization of lignocellulosic fruit waste as an alternative feedstock for bioethanol production. Bioresources 9 (2), 1873–1885.

Oyekanmi, A.A., Ahmad, A., Hossain, K., Id, M.R., 2019. Adsorption of Rhodamine B dye from aqueous solution onto acid treated banana peel : response surface methodology, kinetics and isotherm studies. PLoS ONE 1–20.

Panneerselvam, P., Morad, N., Tan, K.A., 2011. Magnetic nanoparticle (F3O4) impregnated onto tea waste for the removal of nickel(II) from aqueous solution. J. Hazard. Mater. 186 (1), 160–168. doi:10.1016/j.jhazmat.2010.10.102.

Pathak, P.D., Mandavgane, S.A., Kulkarni, B.D., 2017. Fruit peel waste: characterization and its potential uses. Curr. Sci. 113 (3), 444–454. doi:10.18520/cs/v113/i03/444-454.

Portinho, R., Zanella, O., Féris, L.A., 2017. Grape stalk application for caffeine removal through adsorption. J. Environ. Manage. 202, 178–187. doi:10.1016/j.jenvman.2017.07.033.

Quesada, H.B., Baptista, A.T.A., Cusioli, L.F., Seibert, D., de Oliveira Bezerra, C., Bergamasco, R., 2019. Surface water pollution by pharmaceuticals and an alternative of removal by low-cost adsorbents: a review. Chemosphere 222, 766–780. doi:10.1016/j.chemosphere.2019.02.009.

Rigueto, C.V.T., Nazari, M.T., De Souza, C.F., Cadore, J.S., Brião, V.B., Piccin, J.S., 2020. Alternative techniques for caffeine removal from wastewater: an overview of opportunities and challenges. J. Water Process Eng. 35. doi:10.1016/j.jwpe.2020.101231, March.

Sahoo, T.R., Prelot, B., 2020. Adsorption Processes for the Removal of Contaminants from Wastewater: the Perspective Role of Nanomaterials and Nanotechnology. Elsevier Inc..

Shah, A.I., Din Dar, M.U., Bhat, R.A., Singh, J.P., Singh, K., Bhat, S.A., 2020. Prospectives and challenges of wastewater treatment technologies to combat contaminants of emerging concerns. Ecol. Eng. 152, 105882. doi:10.1016/j.ecoleng.2020.105882, April.

Sharma, S., Nandal, P., Arora, A., 2018. Ethanol production from NaOH pretreated rice straw : a cost effective option to manage rice crop residue. Waste Biomass Valoriz. doi:10.1007/s12649-018-0360-4, vol. 0, no. 0, p. 0.

Shebanova, O.N., Lazor, P., 2003. Raman spectroscopic study of magnetite (FeFe2O4): a new assignment for the vibrational spectrum. J. Solid State Chem. 174 (2), 424–430. doi:10.1016/S0022-4596(03)00294-9.

Sotelo, J.L., Ovejero, G., Rodríguez, A., Álvarez, S., Galán, J., García, J., 2014. Competitive adsorption studies of caffeine and diclofenac aqueous solutions by activated carbon. Chem. Eng. J. 240, 443–453. doi:10.1016/j.cej.2013.11.094.

Stavrinou, A., Aggelopoulos, C.A., Tsakiroglou, C.D., 2018. Exploring the adsorption mechanisms of cationic and anionic dyes onto agricultural waste peels of banana, cucumber and potato: adsorption Kinetics and Equilibrium Isotherms as a Tool. Environ. Chem. Eng. doi:10.1016/j.jece.2018.10.063.

Tran, H.N., You, S., Hosseini-bandegharaei, A., Chao, H., 2017. Mistakes and inconsistencies regarding adsorption of contaminants from aqueous solutions: a critical review. Water Res. doi:10.1016/j.watres.2017.04.014.

Zamora-Ledezma, C., et al., May 2021. Heavy metal water pollution: a fresh look about hazards, novel and conventional remediation methods. Environ. Technol. Innov. 22, 101504. doi:10.1016/j.eti.2021.101504.

Zheng, X., et al., 2018. Facile synthesis of Fe 3 O 4 @MOF-100(Fe) magnetic microspheres for the adsorption of diclofenac sodium in aqueous solution. Environ. Sci. Pollut. Res. 25 (31), 31705–31717. doi:10.1007/s11356-018-3134-4.